

1D and 2D End-to-End Azido-Bridged Cobalt(II) Complexes: Syntheses, Crystal Structures, and Magnetic Properties

Morsy A. M. Abu-Youssef,[†] Franz A. Mautner,[‡] and Ramon Vicente^{*§}

Chemistry Department, Faculty of Science, Alexandria University, P. O. Box 426, Ibrahimia, 21321-Alexandria, Egypt, Institut für Physikalische und Theoretische Chemie, Technische Universität Graz, Rechbauerstrasse 12, A-8010 Graz, Austria, and Departament de Química Inorgànica, Universitat de Barcelona, Martí i Franquès 1-11, 08028-Barcelona, Spain

Received November 23, 2006

Two new polynuclear azido-bridged Co(II) compounds with formulas *catena*-[Co($\mu_{1,3}$ -N₃)(N₃)(py)₂(H₂O)]_n (**1**) and [Co($\mu_{1,3}$ -N₃)₂(4-acpy)₂]_n (**2**) (py = pyridine, 4-acpy = 4-acetylpyridine) have been structurally and magnetically characterized. Compound **1** crystallizes in the orthorhombic system *Fddd* space group and consists of a single end-to-end azido-bridged chain with the Co(II) atoms in a CoN₅O slightly distorted octahedron. Compound **2** crystallizes in the monoclinic system *P2₁/a* space group and shows 2D sheets built up through end-to-end azido bridges with the Co(II) atoms in a CoN₆ environment. The magnetic properties of **1** and **2** are reported. In the high-temperature region, the plots of χ_M or $\chi_M T$ vs *T* for **1** and **2** compounds can be fitted by using the Curie–Weiss law, and the best-fit Θ values are –69.1 and –22.6 K, respectively. For **2** magnetic ordering and spontaneous magnetization is achieved below $T_c = 25$ K.

Introduction

The preparation and study of molecule-based magnets have been of considerable interest in recent years with the aim to obtain high- T_c compounds. The usual synthetic approach is to try to build up high-dimensional polynuclear derivatives by mixing paramagnetic centers with suitable bridging and terminal ligands. The paradigmatic bridging ligand is the cyanide one, which has generated a pleiad of high-dimensional systems,^{1–14} some of them with T_c in the range

190–376 K.^{3,4,10,11} The azido ligand is another suitable bridging ligand which shows several coordination bridging modes, the more usual being $\mu_{1,3}$ (end-to-end, EE) or $\mu_{1,1}$ (end-on, EO). With the above-mentioned strategy, by the mixing of Mn(II) salts, azido ligand, and terminal ligands (in some cases no terminal ligand has been added) in solvents like methanol, a great number of crystalline compounds with general formula [Mn(N₃)₂(L)₂]_n have been reported. L is usually a R-pyridine monodentate ligand, or (L)₂ is one bidentate aromatic N-donor ligand. These compounds show all the range of dimensionalities: from 0D to 3D systems.^{15–32}

* To whom correspondence should be addressed. E-mail: ramon.vicente@qi.ub.es. Fax: +34 934907725.

[†] Alexandria University. E-mail: morsy5@link.net. Fax: +2 03 5932488.

[‡] Technische Universität Graz. E-mail: mautner@ptc.tu-graz.ac.at. Fax: +43 316 873 8221.

[§] Universitat de Barcelona.

(1) Ludi, A.; Güdel, H. U. *Struct. Bonding (Berlin)* **1973**, *14*, 1.

(2) Babel, D. *Comments Inorg. Chem.* **1986**, *5*, 285.

(3) Gadet, V.; Mallah, T.; Castro, I.; Veillet, P.; Verdager, M. *J. Am. Chem. Soc.* **1992**, *114*, 9213.

(4) Mallah, T.; Thiébaud, S.; Verdager, M.; Veillet, P. *Science* **1993**, *262*, 1554.

(5) Ferlay, S.; Mallah, T.; Ouahés, R.; Veillet, P.; Verdager, M. *Nature* **1995**, *378*, 701.

(6) Verdager, M.; Bleuzen A.; Marvaud, V.; Vaissermann, J.; Seuleiman, M.; Desplanches, C.; Scuille, A.; Train, C.; Garde, R.; Gelly, G.; Lomenech, C.; Rosenman, I.; Veillet, P.; Cartier, C.; Villain, F. *Coord. Chem. Rev.* **1999**, *190–192*, 1023.

(7) Verdager, M. *Polyhedron* **2001**, *20*, 1115.

(8) Garde, R.; Villain, F.; Verdager, M. *J. Am. Chem. Soc.* **2002**, *124*, 10531.

(9) Dunbar, K. R.; Heintz, R. A. *Prog. Inorg. Chem.* **1997**, *45*, 283.

(10) Entley, W. R.; Girolami, G. S. *Science* **1995**, *268*, 397.

(11) Holmes, S. M.; Girolami, G. S. *J. Am. Chem. Soc.* **1999**, *121*, 5593.

(12) Hatlevik, O.; Buschmann, W. E.; Zhang, J.; Manson, J. L.; Miller, J. S. *Adv. Mater.* **1999**, *11*, 914.

(13) Buschmann, W. E.; Miller, J. S. *Inorg. Chem.* **2000**, *39*, 2411.

(14) Widmann, A.; Kahlert, H.; Petrovic-Prelevic, I.; Wulff, H.; Yakmi, J. V.; Bagkar, N.; Scholz, F. *Inorg. Chem.* **2002**, *41*, 5706.

(15) Ribas, J.; Escuer, A.; Monfort, M.; Vicente, R.; Cortés, R.; Lezama, L.; Rojo, T. *Coord. Chem. Rev.* **1999**, *193–195*, 1027.

(16) Bitschnau, B.; Egger, A.; Escuer, A.; Mautner, F. A.; Sodin, B.; Vicente, R. *Inorg. Chem.* **2006**, *45*, 868 and references therein.

(17) Escuer, A.; Mautner, F. A.; Goher, M. A. S.; Abu-Youssef, M. A. M.; Vicente, R. *Chem. Commun.* **2005**, 605.

(18) Wen, H.-R.; Wang, C.-F.; Song, Y.; Zuo, J.-L.; You, X.-Z. *Inorg. Chem.* **2005**, *44*, 9039.

(19) Abu-Youssef, M. A. M.; Escuer, A.; Vicente, R.; Mautner, F. A.; Ohrstrom, L.; Goher, M. A. S. *Polyhedron* **2005**, *24*, 557.

(20) Gao, E.-Q.; Wang, Z.-M.; Yan, C.-H. *Chem. Commun.* **2003**, 1748.

Furthermore, the ability of the azido bridging ligand to coordinate in $\mu_{1,3}$ (end-to-end, EE) or $\mu_{1,1}$ (end-on, EO) modes, which can be present simultaneously in the same $[\text{Mn}(\text{N}_3)_2(\text{L})_2]_n$ compound, generates a great number of topologies in the 1D and 2D compounds usually obtained. Taking into account that the EE coordination mode typically promotes antiferromagnetic, AF, interactions and the EO coordination mode promotes ferromagnetic, F, interactions, the combination of this fact with the different dimensionalities and topologies found in the $[\text{Mn}(\text{N}_3)_2(\text{L})_2]_n$ compounds gives rise to 1D and 2D systems with a great diversity in their magnetic behavior.

The anisotropic Co(II) is an attractive alternative to the isotropic Mn(II) to obtain azido-bridged 1D–3D compounds with higher T_c or different magnetic properties, taking into account that theoretically the great diversity of dimensionalities and topologies found in the $[\text{Mn}(\text{N}_3)_2(\text{L})_2]_n$ compounds may be obtained for the same $[\text{Co}(\text{N}_3)_2(\text{L})_2]_n$ derivatives. But, as far as we know, surprisingly only a few high-dimensional azido-bridged Co(II) compounds have been described to the date^{33–42} and in some cases the magnetic behavior has not been described.^{33,38,39} In this paper, we report the syntheses and magnetic properties of two new Co(II) end-to-end azido-bridged low-dimensional compounds: the 1D compound *catena*- $[\text{Co}(\mu_{1,3}\text{-N}_3)(\text{N}_3)(\text{py})_2(\text{H}_2\text{O})]_n$ (**1**) and the square-layers 2D compound $[\text{Co}(\mu_{1,3}\text{-N}_3)_2(4\text{-acpy})_2]_n$ (**2**) (py = pyridine, 4-acpy = 4-acetylpyridine). From the point of view of the magnetic properties, **1** and **2** are antiferromagnetically

coupled systems, but for **2** magnetic ordering and spontaneous magnetizations is achieved below $T_c = 25$ K.

Experimental Section

Starting Materials. Cobalt(II) chloride hexahydrate, pyridine, 4-acetylpyridine, L-ascorbic acid, and sodium azide (Aldrich) were used as obtained.

Caution! Azide compounds are potentially explosive! Only a small amount of material should be prepared, and it should be handled with care.

Spectral and Magnetic Measurements. Infrared spectra (4000–200 cm^{-1}) were recorded from KBr pellets on a Perkin-Elmer 380-B spectrophotometer. Magnetic susceptibility measurements under several magnetic fields in the temperature range 2–300 K and magnetization measurements in the field range of 0–5 T were performed with a Quantum Design MPMS-XL SQUID magnetometer at the Magnetochemistry Service of the University of Barcelona. All measurements were performed on polycrystalline samples. Pascal's constants were used to estimate the diamagnetic corrections, which were subtracted from the experimental susceptibilities to give the corrected molar magnetic susceptibilities.

Synthesis. catena- $[\text{Co}(\mu_{1,3}\text{-N}_3)(\text{N}_3)(\text{py})_2(\text{H}_2\text{O})]_n$ (1**).** To a 15 cm^3 aqueous solution of $\text{CoCl}_2 \cdot 6\text{H}_2\text{O}$ (0.48 g, 2 mmol) was added a 10 cm^3 solution of pyridine (0.65 g, 8.2 mmol) in ethanol followed by few drops of a saturated aqueous solution of L-ascorbic acid. Further, a 10 cm^3 aqueous solution of NaN_3 (0.65 g, 10 mmol) was added drop by drop with continuous stirring. The clear pink solution was allowed to stand at room temperature for a couple of days. Deep pink crystals of *catena*- $[\text{Co}(\mu_{1,3}\text{-N}_3)(\text{N}_3)(\text{py})_2(\text{H}_2\text{O})]_n$ (**1**) were obtained which were suitable for X-ray measurements, with a yield 0.50 g, ~64% with respect to metal. Anal. Found (calcd): C, 37.4 (37.6); H, 3.9 (3.8); N, 35.4 (35.1); Co, 18.3 (18.5). IR spectrum as KBr pellets (cm^{-1}) (v, very; s, strong; m, medium; w, weak; br, broad): 3434 s, 3369 s, 2073 vs, 1643 w, 1598 s, 1484 ms, 1441 s, 1212 ms, 1142 ms, 1072 s, 1039 s, 1010 ms, 755 ms, 697 s, 662 w, 628 m, 593 m, 411 w, 387 w, 365 w, 342 m, 315 ms, 293 ms, 269 s, 234 vs.

$[\text{Co}(\mu_{1,3}\text{-N}_3)_2(4\text{-acpy})_2]_n$ (2**).** was synthesized by mixing a solution of 4-acetylpyridine (0.5 mL, 4.46 mmol) in 5.0 mL ethanol with a solution of $\text{CoCl}_2 \cdot 6\text{H}_2\text{O}$ (0.48 g, ~2.0 mmol) in 10 mL ethanol and few drops of an aqueous saturated solution of L-ascorbic acid, followed by drop by drop addition of an aqueous solution (2 mL) of NaN_3 (0.32 g, ~5.0 mmol) with constant stirring. The red mixture was allowed to stand at room temperature for several days until good quality pink crystals of the complex **2** were obtained with a yield of 0.58 g, ~75% with respect to metal. Anal. Found (calcd): C, 43.4 (43.6); H, 3.5 (3.7); N, 29.4 (29.1); Co, 15.2 (15.3). IR spectrum as KBr pellets (cm^{-1}): 3403 w, 3071 w, 2076 vs, 1699 vs, 1645 w, 1610 w, 1553 m, 1408 s, 1363 ms, 1322 w, 1265 s, 1257 s, 1228 ms, 1062 w, 1015 w, 961 w, 871 vw, 824 ms, 664 w, 627 w, 582 s, 461 w, 432 w, 409 w, 387 w, 366 w, 315 w, 291 m, 270 s.

X-ray Crystallography. The X-ray single-crystal data were collected on a modified STOE 4 circle diffractometer with graphite-monochromated $\text{Mo K}\alpha$ radiation ($\lambda = 0.71069 \text{ \AA}$). The crystallographic conditions retained for the intensity data collection, and some features of the structure refinements are listed in Table 1. Lorentz–polarization and absorption corrections were made using the DIFABS computer program.⁴³ The structures were solved by direct methods using the SHELXS-86⁴⁴ computer program and refined by full-matrix least-squares methods on F^2 , using the

- (21) Gao, E.-Q.; Cheng, A.-L.; Xu, Y.-X.; He, M.-Y.; Yan, C.-H. *Inorg. Chem.* **2005**, *44*, 8822.
- (22) Zhao, W.; Song, Y.; Okamura, T.; Fan, J.; Sun, W.-Y.; Ueyama, N. *Inorg. Chem.* **2005**, *44*, 3330.
- (23) Ni, Z.-H.; Kou, H.-Z.; Zheng, L.; Zhao, Y.-H.; Zhang, L.-F.; Wang, R.-J.; Cui, A.-L.; Sato, O. *Inorg. Chem.* **2005**, *44*, 4728.
- (24) Ghosh, A. K.; Ghoshal, D.; Zangrando, E.; Ribas, J.; Chaudhuri, N. R. *Inorg. Chem.* **2005**, *44*, 1786.
- (25) Wang, X.-Y.; Li, B.-L.; Zhu, X.; Gao, S. *Eur. J. Inorg. Chem.* **2005**, 3277.
- (26) Abu-Youssef, M. A. M.; Escuer, A.; Langer, V. *Eur. J. Inorg. Chem.* **2005**, 4659.
- (27) Abu-Youssef, M. A. M.; Escuer, A.; Langer, V. *Eur. J. Inorg. Chem.* **2006**, 3177.
- (28) He, Z.; Wang, Z.-M.; Gao, S.; Yan, C. H. *Inorg. Chem.* **2006**, *45*, 6694.
- (29) Das, A.; Rosair, G. M.; Salah El Fallah, M.; Ribas, J.; Mitra, S. *Inorg. Chem.* **2006**, *45*, 3301.
- (30) Bai, S.-Q.; Gao, E.-Q.; He, Z.; Fang, C.-J.; Yue, Y.-F.; Yan, C.-H. *Eur. J. Inorg. Chem.* **2006**, 407.
- (31) Escuer, A.; Vicente, R.; Goher, M. A. S.; Mautner, F. A. *Inorg. Chem.* **1995**, *34*, 5707.
- (32) Escuer, A.; Vicente, R.; Goher, M. A. S.; Mautner, F. A. *Inorg. Chem.* **1997**, *36*, 3440.
- (33) Goher, M. A. S.; Mautner, F. A. *Polyhedron* **1999**, *18*, 2339.
- (34) Hong, C. S.; Koo, J.-e.; Son, S.-K.; Lee, Y.-S.; Kim, Y.-S.; Do, Y. *Chem.–Eur. J.* **2001**, *7*, 4243.
- (35) Liu, T.-F.; Fu, D.; Gao, S.; Zhang, Y.-Z.; Sun, H.-L.; Su, G.; Liu, Y.-J. *J. Am. Chem. Soc.* **2003**, *125*, 13976.
- (36) Viau, G.; Lombardi, M. G.; De Mundo, G.; Julve, M.; Lloret, F.; Faus, J.; Caneschi, A.; Clemente-Juan, J. M. *Chem. Commun.* **1997**, 1195.
- (37) Doi, Y.; Ishida, T.; Nogami, T. *Bull. Chem. Soc. Jpn.* **2002**, *75*, 2455.
- (38) Chen, H.-J.; Chen, X.-M.; Zhou, D.-Y.; Zhou, Y.-C. *Supramol. Chem.* **2002**, *14*, 21.
- (39) You, z.-L. *Acta Crystallogr., Sect. C: Cryst. Struct. Commun.* **2005**, *61*, m295.
- (40) Wang, X.-Y.; Wang, L.; Wang, Z.-M.; Gao, S. *J. Am. Chem. Soc.* **2006**, *128*, 674.
- (41) Li, X.-J.; Wang, X.-Y.; Gao, S.; Cao, R. *Inorg. Chem.* **2006**, *45*, 1508.
- (42) Liu, T.; Zhang, Y.; Wang, Z.; Gao, S. *Inorg. Chem.* **2006**, *45*, 2782.

- (43) Walker, N.; Stuart, D. *Acta Crystallogr.* **1983**, *A39*, 158.

Table 1. Crystal and Structure Refinement Data for Complexes *catena*-[Co($\mu_{1,3}$ -N₃)(N₃)(py)₂(H₂O)]_n (**1**) and [Co($\mu_{1,3}$ -N₃)₂(4-acpy)₂]_n (**2**)

param	1	2
formula	C ₁₀ H ₁₂ CoN ₈ O	C ₁₄ H ₁₄ CoN ₈ O ₂
mol wt	319.21	358.26
system	orthorhombic	monoclinic
space group	Fddd	P2 ₁ /a
a/Å	10.642(3)	8.045(3)
b/Å	16.477(5)	8.335(3)
c/Å	29.817(8)	11.588(4)
α/deg	90	90
β/deg	90	93.22(3)
γ/deg	90	90
V/Å ³	5228(3)	775.8(5)
Z	16	2
T/K	99(2)	99(2)
μ _{MoKα} /mm ⁻¹	1.323	1.135
ρ _{calc} /Mg m ⁻³	1.622	1.649
cryst size/mm ³	0.52 × 0.30 × 0.20	0.36 × 0.20 × 0.08
θ _{max} /deg	30.00	26.99
data colld	2103	2183
indepd reflns/R _{int}	1910/0.0240	1702/0.0318
params	109	116
goodness-of-fit on F ²	1.056	1.1088
R1/wR2 (all data)	0.0376/0.1050	0.0408/0.0950
resid electron density/e Å ⁻³	0.812/−0.473	0.366/−0.328

SHELXL-93⁴⁵ program incorporated in the SHELXTL/PC V 5.03⁴⁶ program package. All non-hydrogen atoms were refined anisotropically. The hydrogen atoms were assigned with isotropic displacement factors and included in the final refinement cycles by use of geometrical restraints ($C_{ar} = 0.93$ Å, $C_{Me} = 0.96$ Å, O–H = 0.82 Å). In case of **1**, occupancies of 0.5 were applied to disordered atoms of aqua ligand and monodentate N(21)–N(22)–N(23) azide group. Molecular plots were obtained with the ORTEP-3 graphic program.⁴⁷

Results and Discussion

The results of elemental analyses and IR spectra for **1** indicate that the reaction between cobalt(II) ions and pyridine in presence of azide ions, in aqueous/ethanolic solution, afforded deep pink crystals of a 1:2:2 complex, respectively, with the formula *catena*-[Co($\mu_{1,3}$ -N₃)(N₃)(py)₂(H₂O)]_n. Further, a water molecule was coordinated to the Co(II) ion alternating to the terminal azide group giving rise to a 2D H-bonded structure which was indicated through strong bands at 3434 and 3369 cm⁻¹ in the IR spectra. L-Ascorbic acid was added to avoid the spontaneous oxidation of Co(II) ions by air. In case of using 4-acetylpyridine instead of pyridine, pink crystals with higher yield percentage of **2** with the ratio 1:2:2 and formula [Co($\mu_{1,3}$ -N₃)₂(4-acpy)₂]_n were obtained. The IR spectra of both complexes **1** and **2** reveal the presence of the coordinated azide ions with very strong bands at 2073 and 2076 cm⁻¹ for the antisymmetric vibrations and at 1212 and 1228 cm⁻¹ for symmetric vibrations, respectively. The ring breathing vibration of the pyridine moiety at 1000 cm⁻¹ was shifted in the IR spectra of

crystalline complexes to 1015 and 1010 cm⁻¹ for **1** and **2**, respectively. Also the M–N(L) and M–N(N₃) vibrations were recognized in the range 293–234 cm⁻¹. Both complexes **1** and **2** are insoluble in most solvents, indicating their polymeric nature.

Description of the Structures. A perspective view of a fragment of the 1-D system of *catena*-[Co($\mu_{1,3}$ -N₃)(N₃)(py)₂(H₂O)]_n (**1**), together with the atom-labeling scheme, is given in Figure 1a, and selected bond parameters are summarized in Table 2. The neutral complex crystallizes in the orthorhombic space group *Fddd*, with 16 formulas/unit cell. The Co(1) center and both pyridine ligands are located at special position 16g, and the bridging azide group is located on special position 16f (i.e., diades). The disordered monodentate azide group and also the disordered aqua ligand are located on general positions (32h) and have a split occupancy of 0.5.

The Co(1) center is six-coordinated with a slightly elongated trans-octahedral geometry. The equatorial sites of the octahedron are occupied by N(1) and N(2) of the two pyridine ligands [Co(1)–N(1) = 2.157(3), Co(1)–N(2) = 2.147(3) Å, N(1)–Co(1)–N(2) = 180.0°]. Two equatorial sites of the polyhedron are occupied by N(11) and N(11A) of symmetry-related μ -1,3 single azide bridges [Co(1)–N(11) = 2.103(2) Å, N(11)–Co(1)–N(11A) = 179.77(12)°]. These μ -1,3 single azido bridges connect the Co(1) polyhedra to a 1D chain oriented along the *a*-axis of the unit cell. The remaining two equatorial sites are statistically occupied by N(21) of a monodentate azide group and O(1) of an aqua ligand [Co(1)–N(21)/O(1) = 2.114(2) Å, N(21A)–Co(1)–O(1) = 178.38(11)°]. The bond parameters of the μ -1,3 azido bridge are N(11)–N(12) = 1.163(2) Å, N(11)–N(12)–N(11A) = 177.0(3)°, and Co(1)–N(11)–N(12) = 132.8(2)°, whereas the corresponding values of the monodentate azide ligand are N(21)–N(22) = 1.243(4) Å, N(22)–N(23) = 1.146(5) Å, N(21)–N(22)–N(23) = 176.7(6)°, and Co(1)–N(21)–N(22) = 122.8(2)°. The Co(1)⋯Co(1D) intrachain distance is 5.3877(16) Å, the Co(1C)⋯Co(1)⋯Co(1D) angle is 162.0(3)°, and the Co(1)–N(11)⋯N(11B)–Co(1D) torsion angle is 45.6(4)°. The equatorial CoN₃O planes of adjacent polyhedra are oriented parallel. The interplanar angle of two trans-coordinated pyridine rings at the same Co(1) center is 121.0(3)°, whereas pyridine rings of two neighboring Co(1) centers form interplanar angles of 94.9(4)°. There exists two kinds of hydrogen bonds of type O–H⋯N. Intrachain hydrogen bonds are formed between O(1) and N(21) atoms of monodentate azide groups [O(1)⋯N(21') = 2.792(6), H(7)⋯N(21') = 1.984 Å; O(1)–H(7)⋯N(21') = 169.6°]. Interchain hydrogen bonds from O(1) to N(23') atoms of adjacent chains of Co(1) polyhedra [O(1)⋯N(23'') = 2.857(6), H(8)⋯N(23'') = 1.579 Å; O(1)–H(8)⋯N(23'') = 168.6, N(21')⋯O(1)⋯N(23'') = 100.0(4)°] further extend the 1D system to supramolecular 2D layers parallel to the *ab*-plane of the unit cell (Figure 1b). The Co(1)⋯Co(1E) interchain distance is 8.232(3) Å. These supramolecular layers are separated by the *trans*-pyridine

(44) Sheldrick, G. M. *SHELXS-86, Program for the Solution of Crystal Structure*; University of Goettingen: Goettingen, Germany, 1986.

(45) Sheldrick, G. M. *SHELXL-93, Program for the Refinement of Crystal Structure*; University of Goettingen: Goettingen, Germany, 1993.

(46) *SHELXTL 5.03 (PC-Version), Program library for the Solution and Molecular Graphics*; Siemens Analytical Instruments Division: Madison, WI, 1995.

(47) ORTEP-3 for Windows: Farrugia, L. J. *J. Appl. Crystallogr.* **1997**, *30*, 565.

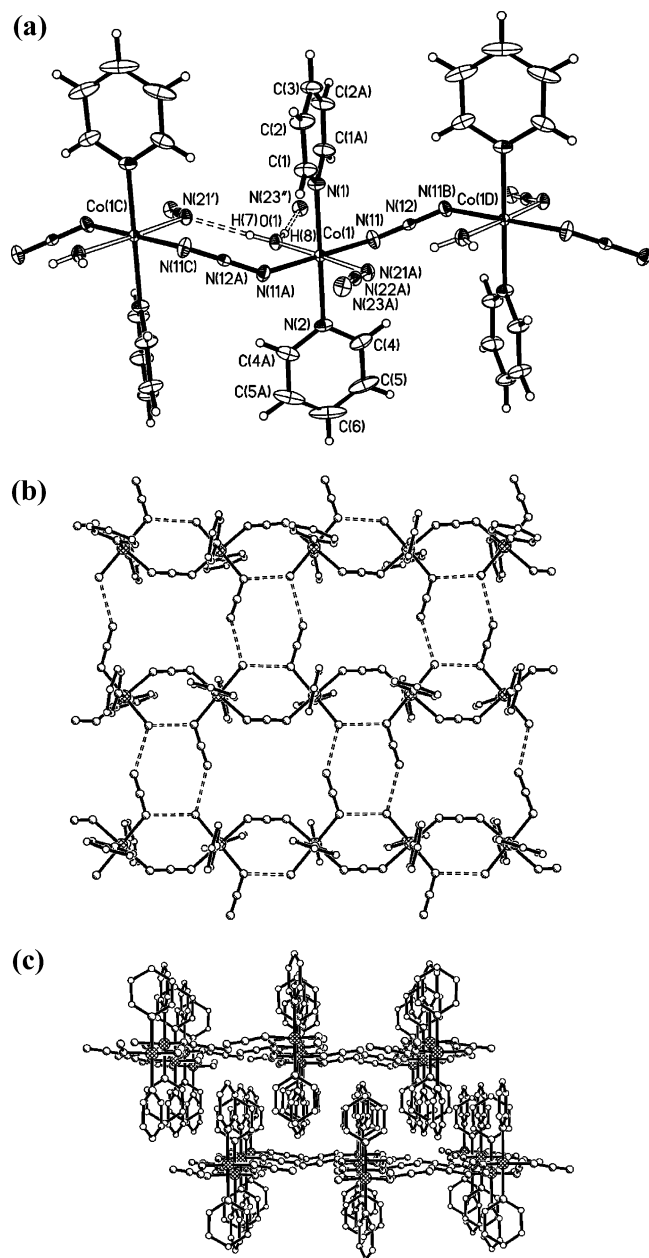


Figure 1. (a) ORTEP view (40% probability ellipsoids) of a fragment of the *catena*-[Co($\mu_{1,3}$ -N₃)(N₃)(py)₂(H₂O)]_n (**1**) 1D chain system together with the atom-labeling scheme. Symmetry codes: (A) $0.75 - x, 0.75 - y, z$; (B) $0.25 - x, y, 0.25 - z$; (C) $0.50 + x, 0.75 - y, 0.25 - z$; (D) $-0.50 + x, 0.75 - y, 0.25 - z$; (E) $0.75 - x, 0.50 + y, 0.25 - z$. Disordered aqua ligands and monodentate azide groups with occupancy 0.5 are indicated by open stick bonds and O—H...N hydrogen bonds by broken bonds. (b) Supramolecular layers formed by hydrogen bonds of type O—H...N (indicated by broken bonds) viewed along the *c*-axis of the unit cell. Disordered aqua and azide ligands may be interchanged in a statistical manner. (c) Packing view of two supramolecular sheets of **1** viewed along the *a*-axis of the unit cell.

ligands, with an interplane distance of 7.454(3) Å, which corresponds with 1/4 of the *c*-axis of the unit cell (Figure 1c).

A perspective view together with the atom-labeling scheme of complex **2** is shown in Figure 2a; selected bond distances and bond angles are listed in Table 3. The structure consists of an extended two-dimensional layer of octahedrally coordinated centrosymmetric cobalt atoms, bridged by means of μ -1,3-azide ligands (Figure 2b). Each cobalt atom has two

Table 2. Selected Bond Lengths (Å) and Bond Angles (deg) for *catena*-[Co($\mu_{1,3}$ -N₃)(N₃)(py)₂(H₂O)]_n (**1**)^a

Co(1)—N(1)	2.157(3)	Co(2)—N(2)	2.147(3)
Co(1)—N(11)	2.103(2)	Co(1)—O(1)	2.114(2)
Co(1)—N(21)	2.114(2)	N(11)—N(12)	1.163(2)
N(21)—N(22)	1.243(4)	N(22)—N(23)	1.146(5)
Co(1)···Co(1C)	5.3877(16)	Co(1)···Co(1E)	8.282(3)
N(1)—Co(1)—N(2)	180.0	N(11)—Co(1)—N(11A)	179.77(12)
N(21)—Co(1)—O(1)	178.38(11)	N(1)—Co(1)—O(1)	90.81(5)
N(2)—Co(1)—N(21A)	89.19(5)	N(11)—Co(1)—N(2)	89.89(6)
N(11A)—Co(1)—N(21)	92.00(8)	N(11)—Co(1)—O(1)	88.00(8)
Co(1)—N(11)—N(12)	132.8(2)	N(11)—N(12)—N(11B)	177.0(3)
Co(1)—N(21)—N(22)	122.8(2)	N(21)—N(22)—N(23)	176.7(6)
Co(1C)···Co(1)···Co(1D)	162.0(2)		

^a Symmetry code: (A) $0.75 - x, 0.75 - y, z$; (B) $0.25 - x, y, 0.25 - z$; (C) $0.50 + x, 0.75 - y, 0.25 - z$; (D) $-0.50 + x, 0.75 - y, 0.25 - z$; (E) $0.75 - x, 0.50 + y, 0.25 - z$.

Table 3. Selected Bond Lengths (Å) and Bond Angles (deg) for [Co($\mu_{1,3}$ -N₃)₂(4-*acpy*)₂]_n (**2**)^a

Co(1)—N(11)	2.109(2)	Cu(1)—N(13)	2.131(2)
Co(1)—N(1)	2.159(2)	Co(1)···Co(1B)	5.792(2)
N(11)—N(12)	1.168(3)	N(12)—N(13B)	1.184(3)
N(11)—Cu(1)—N(13)	90.92(10)	N(11)—Co(1)—N(1)	91.85(9)
N(13)—Co(1)—N(1A)	90.23(9)	Co(1)—N(11)—N(12)	146.6(2)
N(11)—N(12)—N(13B)	176.7(3)	Co(1)—N(13)—N(12C)	126.6(2)

^a Symmetry code: (A) $-x, -y, -z$; (B) $1/2 - x, -1/2 + y, -z$; (C) $1/2 - x, 1/2 + y, -z$.

4-acetylpyridine ligands coordinated by means of the nitrogen atom of the pyridyl group in a *trans*-arrangement and four azide ligands in the equatorial plane. The axial Co(1)—N(1) bond length is 2.159(2) Å, whereas the shorter Co—N(azido)-bond distances are Co(1)—N(11) 2.109(2) and Co(1)—N(13) 2.131(2) Å. Each of the four azide ligands acts as a μ -1,3 bridge with each one of the neighboring cobalt atoms to form a two-dimensional square layer. The Co(1)—N(11)—N(12) and Co(1B)—N(13B)—N(12) bond angles of 146.6(2) and 126.6(2)°, respectively, are in the usual M—N—N range found for μ -1,3 bridges with Cu(II), Ni(II), or Mn(II) polynuclear compounds. The Co(1)—N(11)···N(13B)—Co(1B) torsion angle is $-89.3(3)$ °. The acute interplanar angle between neighboring CoN₄(azido) planes is 83.81(7)°. The Co(1)···Co(1B) intraplane distance is 5.792(2) Å. The layers are separated by the *trans*-4-acetylpyridine ligands, with an interplane distance of 11.588(5) Å, which corresponds with the *c*-axis of the unit cell (Figure 2c). The Mn(II) compound with the same formula, [Mn($\mu_{1,3}$ -N₃)₂(4-*acpy*)₂]_n, has also the same square layer structure³¹ with Mn—N—N bond angles of 151.6(2) and 129.0(2)° and an Mn—N₃—Mn torsion angle of 81.9°. The minimum interlayer Mn···Mn distance is similar: 11.563(5)°.

Magnetic Data. The magnetic properties of **1**, in the form of $\chi_M T$ vs *T*, are represented in Figure 3. The $\chi_M T$ vs *T* values are not field dependent. The $\chi_M T$ value at 300 K is equal at 3.04 cm³ mol⁻¹ K, which is higher than the spin-only value (1.875 cm³ K mol⁻¹) for an uncoupled *S* = 3/2 Co(II) ion, in accordance with the usual orbital contribution of the octahedral Co(II) ions. On lowering of the temperature, the $\chi_M T$ value decreases gradually to a value of 0.22 cm³ mol⁻¹ K at 2 K. No maximum is found in the χ_M vs *T* plot. The magnetic susceptibility in the 25–300 K range obeys the

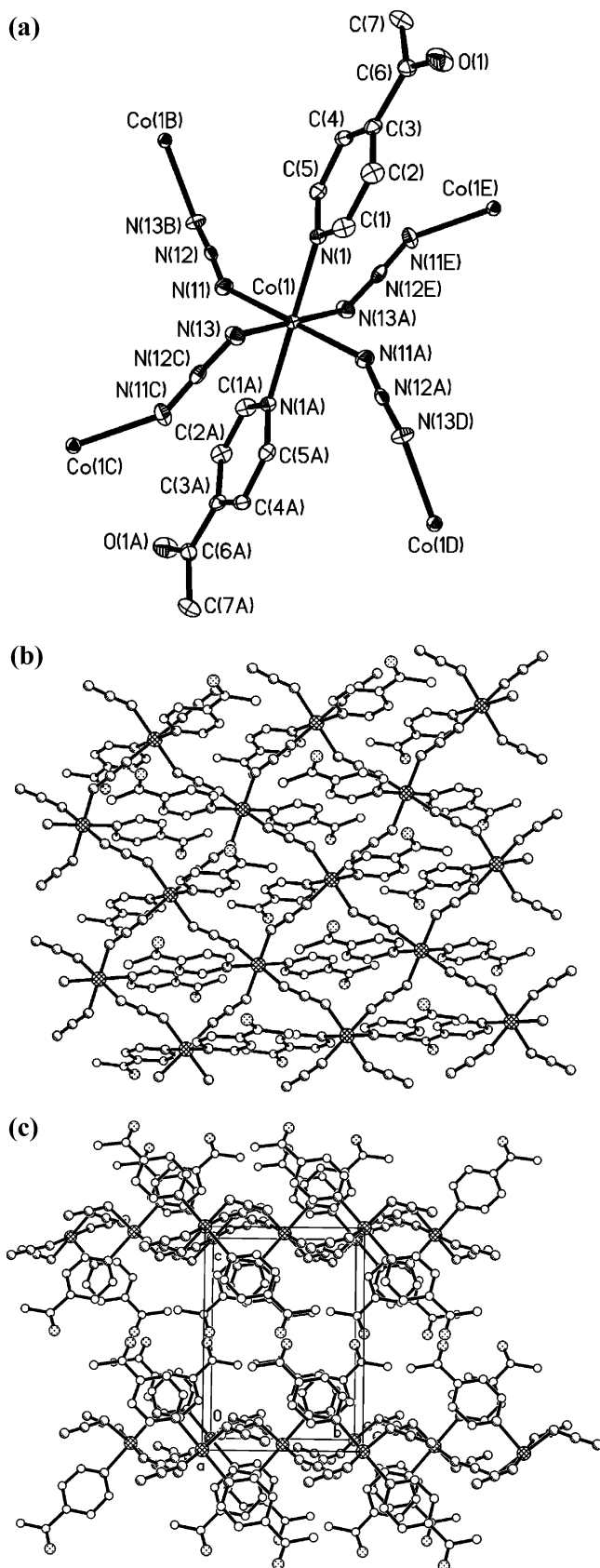


Figure 2. (a) Ortep view (40% probability ellipsoids) and atom-labeling scheme of $[\text{Co}(\mu_{1,3}\text{-N}_3)_2(4\text{-acpy})_2]_n$ (**2**). Symmetry codes: (A) $-x, -y, -z$; (B) $1/2 - x, -1/2 + y, -z$; (C) $1/2 - x, 1/2 + y, -z$; (D) $-1/2 + x, 1/2 - y, z$; (E) $-1/2 + x, -1/2 - y, z$; (F) $1/2 + x, -1/2 - y, z$. (b) 2D layers system of **2** viewed along the c -axis of the unit cell. (c) Packing view of **2** along the a -axis of the unit cell.

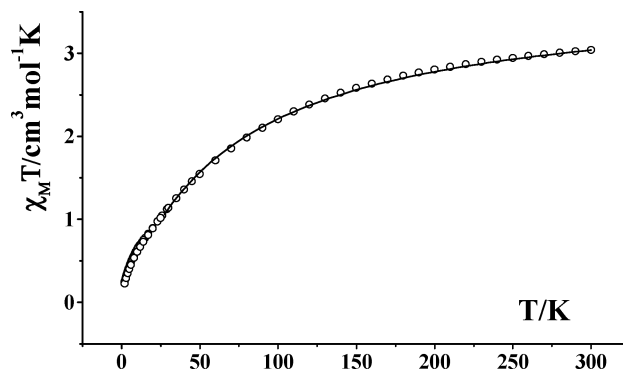


Figure 3. Plot of $\chi_M T$ vs T in the 300–2 K range of temperatures for $\text{catena-}[\text{Co}(\mu_{1,3}\text{-N}_3)(\text{N}_3)(\text{py})_2(\text{H}_2\text{O})]_n$ (**1**). The solid line shows the best fit as Curie–Weiss law (see text).

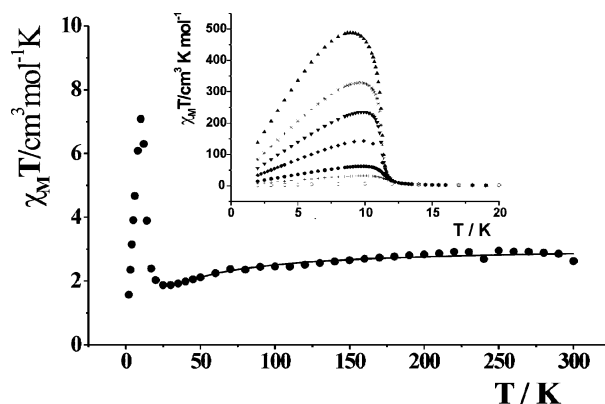


Figure 4. Plot of $\chi_M T$ vs T in the 300–2 K range of temperatures for $[\text{Co}(\mu_{1,3}\text{-N}_3)_2(4\text{-acpy})_2]_n$ (**2**) measured under external magnetic field of 5000 G. The solid line shows the best fit in the high-temperature region as Curie–Weiss law (see text). Inset: Plot of $\chi_M T$ vs T in the 20–2 K range of temperatures for **2** measured under external magnetic fields of 20, 50, 100, 200, 500, 1000, and 5000 G (from top to bottom in the plot).

Curie–Weiss law ($\chi_M = C/(T - \Theta)$) with a Curie constant $C = 3.74 \text{ cm}^3 \text{ mol}^{-1} \text{ K}$ and $\Theta = -69.1 \text{ K}$.

The magnetic properties of **2**, in the form of $\chi_M T$ vs T , are represented for the values of the applied magnetic field of 20, 50, 100, 200, 500, 1000, and 5000 G (Figure 4). The room-temperature $\chi_M T$ value of $2.62 \text{ cm}^3 \text{ mol}^{-1} \text{ K}$ is larger than the spin-only value of $1.875 \text{ cm}^3 \text{ mol}^{-1} \text{ K}$ for an uncoupled $S = 3/2$ Co(II) ion. Upon lowering of the temperature, $\chi_M T$ decreases, attains a minimum at 25 K ($\chi_M T = 1.87 \text{ cm}^3 \text{ mol}^{-1} \text{ K}$), and shows an abrupt increase to a maximum value of $7 \text{ cm}^3 \text{ mol}^{-1} \text{ K}$ at 10 K (5000 G) before decreasing in the lowest temperature region. At the same temperature, the $\chi_M T$ value is $443 \text{ cm}^3 \text{ mol}^{-1} \text{ K}$ at the applied field of 20 G. The magnetic susceptibility in the 50–300 K range obeys the Curie–Weiss law with a Curie constant $C = 3.07 \text{ cm}^3 \text{ mol}^{-1}$ and $\Theta = -22.6 \text{ K}$. The continuous decrease in $\chi_M T$ from room temperature to 25 K can be attributed to both the spin–orbit coupling of the octahedral Co(II) ions with a ${}^4\text{T}_{1g}$ ground term and the moderate antiferromagnetic coupling between the Co(II) centers through the $\mu_{1,3}$ -azido bridging ligands. Below 25 K, where an abrupt increase in $\chi_M T$ vs T is observed, the susceptibility becomes field dependent, thus suggesting a ferromagnetic phase transition. At 2 K, **2** exhibits a magnetic hysteresis loop (Figure 5) with a coercitive field of 500 G and a remnant

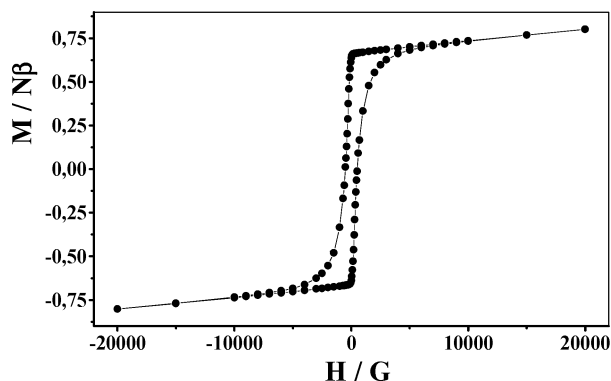


Figure 5. M - H curve of $[\text{Co}(\mu_{1,3}\text{-N}_3)_2(4\text{-acpy})_2]_n$ (**2**) measured at 2 K.

magnetization of $0.64 N\beta$. The magnetization at 2 K attains a highest value at 5 T of $1 N\beta$, which is significantly below the theoretical saturation magnetization of $3 N\beta$ for an isotropic high-spin Co(II).

The reported magnetic properties (negative Weiss constant, hysteresis loop at 2 K, abrupt increase in $\chi_M T$ vs T below 25 K, and no saturation limit) are characteristic of spin canted antiferromagnetism, leading to weak ferromagnetism.^{48,49} The observed spin canting may be attributed to the single ion magnetic anisotropy of the octahedral Co(II) ions and to the systematic alternation of the relative orientation of adjacent metal chromophores:⁴⁹ in the case of **2** the pyridine rings of two neighboring Co(II) centers form interplanar angles of $83.81(7)^\circ$ (see above), this latter feature being typical of some of these canted systems. The 3D long-range

order in **2** is only possible through dipolar and other weak interlayer interactions, and this is the reason for which T_c is relatively low.⁴⁹ With the same structure, the related Mn(II) compound $[\text{Mn}(\mu\text{-N}_3)_2(4\text{-acpy})_2]_n$ shows also magnetic ordering with $T_c = 28$ K.³²

Conclusion

In this work we have synthesized and characterized two new azido-bridged low-dimensional compounds derived from the anisotropic Co(II) with the same strategy used to prepare the related $[\text{Mn}(\text{N}_3)_2(\text{L})_2]_n$ compounds (L is usually a R-pyridine monodentate ligand): by mixing Co(II) salts, azido ligand, and pyridine or 4-acetylpyridine we have synthesized the 1D *catena*- $[\text{Co}(\mu_{1,3}\text{-N}_3)(\text{N}_3)(\text{py})_2(\text{H}_2\text{O})]_n$ (**1**) or the 2D $[\text{Co}(\mu_{1,3}\text{-N}_3)_2(4\text{-acpy})_2]_n$ (**2**) compounds, respectively. In both cases, L-ascorbic acid was used to prevent the oxidation of the Co(II) cations. From the magnetic point of view, in the high-temperature region, **1** and **2** obey the Curie–Weiss law. On the other hand, **2** has the same structure as the related $[\text{Mn}(\mu_{1,3}\text{-N}_3)_2(4\text{-acpy})_2]_n$ compound and they show magnetic ordering at low temperature due to the canting effect.

Acknowledgment. This research was partially supported by the CICYT (Grant CTQ2006-01759) and SIDA (Grant No. 348-2002-6879). F.A.M. thanks B. Sodin (TU-Graz) and Profs. C. Kratky and F. Belaj (University Graz) for assistance.

Supporting Information Available: Tables of X-ray crystallographic data in CIF format for the structures reported in this paper. This material is available free of charge via the Internet at <http://pubs.acs.org>.

IC0622297

(48) Retting, S. J.; Thompson, R. C.; Trotter, J.; Xia, S. *Inorg. Chem.* **1999**, *38*, 1360.

(49) Rodríguez, A.; Kivekäs, R.; Colacio, E. *Chem. Commun.* **2005**, 5228.